WO_3 anchored Fe single-atom composite for efficient photo−Fenton degradation of organic pollutants

Xia Gong,[a] Quanquan Shi,[a*] Huan Li,[b] Guichen Ping,[a] Jinmei Li,[a] Alfons Baiker,[c] Gao Li[b*]

[a] College of Science, Inner Mongolia Agricultural University, Hohhot 010018, China

[b] School of Chemistry and Chemical Engineering, Inner Mongolia Normal University, Hohhot 010018, China

[c] Department of Chemistry and Applied Biosciences, ETH-Zurich, Hönggerberg, HCI, CH-8093 Zurich, Switzerland

*Corresponding authors. E-mail address: qqshi@imau.edu.cn (Q. Shi); li_gao82@yeah.net (G. Li); baiker@chem.ethz.ch (A. Baiker)

Chemicals

Sodium tungstate dihydrate ($Na_2WO_4•2H_2O$), citric acid, glucose, ferric chloride ($FeCl_3•2H_2O$), and tetracycline were purchased from Aldrich. All chemicals were commercially available as reagent grade and used as received without further purification.

Characterization

Powder X-ray diffraction (XRD) patterns were performed using a PANalytical Empyream diffractometer operated at 40 kV and 200 mA. Transmission electron microscopy (TEM) images were recorded using a field-emission transmission electron microscope (FEI Tecnai F20). HAADF-STEM images were obtained using a Thermo Fisher Scientific Themis Z (3.2) instrument. Nitrogen adsorption-desorption isotherms were measured at 77K with a BSD-PS2-1598-A Specific Surface Area & Pore Size Analyzer and specific surface areas were determined using the Brunauer-Emmett-Teller (BET) method. The samples were degassed at 150 °C for 4 hours under vacuum before the BET measurement. UV-visible diffuse reflectance spectra were recorded in the 200–800 nm range using a spectrophotometer (PE Lambda 850) with $BaSO_4$ as the reference. A single-frequency line at 532 nm from a diode-pumped solid-state (DPSS) laser was used as the excitation source. Photoluminescence (PL) spectra and time-resolved photoluminescence (TRPL) spectra were obtained at room temperature on a fluorescence lifetime spectrophotometer (Edinburgh Instruments FS5), excited at 450 nm wavelength. The

photoelectrochemical tests of the samples were performed on an electrochemical workstation (CHI760E, Shanghai) using a standard three-electrode system, consisting of an Ag/AgCl electrode and a Pt plate as the reference and counter electrodes, respectively. The as prepared samples were coated onto FTO glass substrates to serve as the working electrodes. A 300 W Xe lamp with a cut-off filter ($\lambda > 420$ nm) was used as the light source, and all electrochemical tests were carried out in a 0.5 M KH_2PO_3–K_2HPO_3 buffer solution (pH 7). X-ray photoelectron spectra (XPS) were measured on an ESCALAB MK-II spectrometer (VG Scientific Ltd., UK) with Al Kα radiation. Samples were purged in the instrument's pre-chamber at ambient temperature and up to $< 10^{-12}$ bar pressure before the measurements. The charging effect was corrected by adjusting the binding energy of C1s to 284.6 eV. The spectra were deconvoluted using the XPSPEAK program by curve fitting with mixed Gaussian–Lorentzian peaks. Electron spin resonance (ESR) was carried out to determine the $\bullet O^{2-}$ and·•OH radicals with 5,5-dimethyl-1-pyrroline-N-oxide (DMPO) as the spin-trapping agent. Briefly, 10 mg samples were dispersed into 0.5 mL methanol containing 0.05 M DMPO. A 300 W Xe lamp with a cut-off filter ($\lambda > 420$ nm) was used as the light source. After being illuminated for 5 min, ESR signals were recorded by putting the mixture on a Bruker A300 Spectrometer. Electron paramagnetic resonance (EPR) analysis was performed on a Bruker EMXnano spectrometer at room temperature, operating at the X band (~9.8 GHz). The magnetic field was modulated at 100 kHz, and the g value was determined from the precise frequency and magnetic field values.

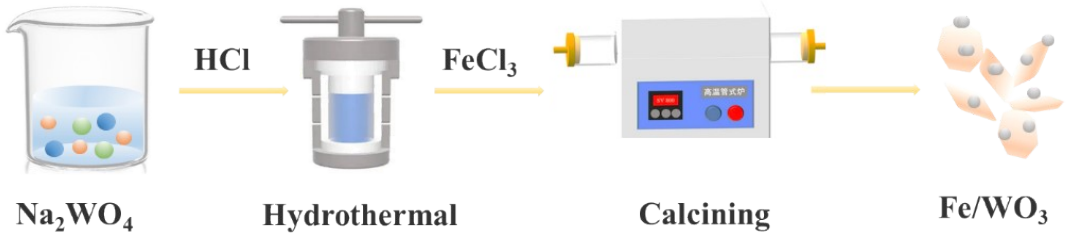

Fig. S1. Schematic diagram of the Fe/WO_3 preparation.

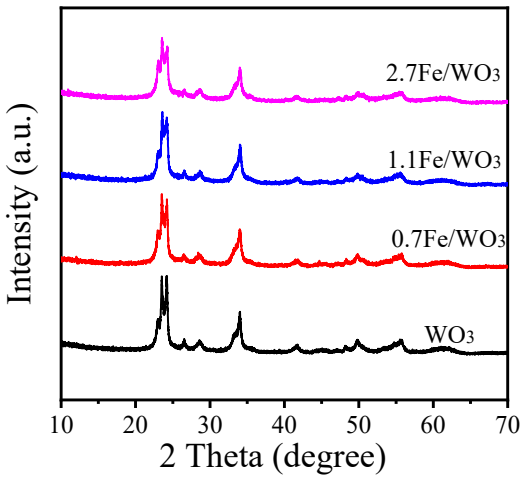

Fig. S2. XRD patterns of WO_3 and Fe/WO_3 samples.

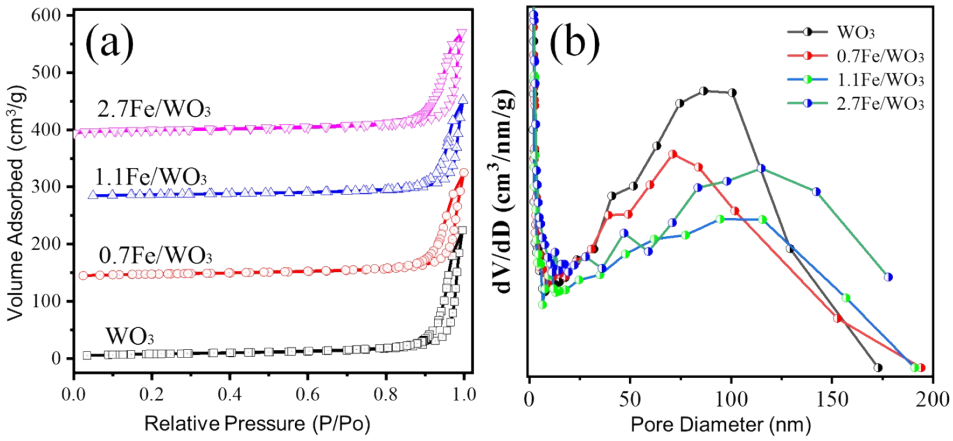

Fig. S3. (a) N_2 adsorption and desorption isotherms and (b) pore size distribution of WO_3 and Fe/WO_3.

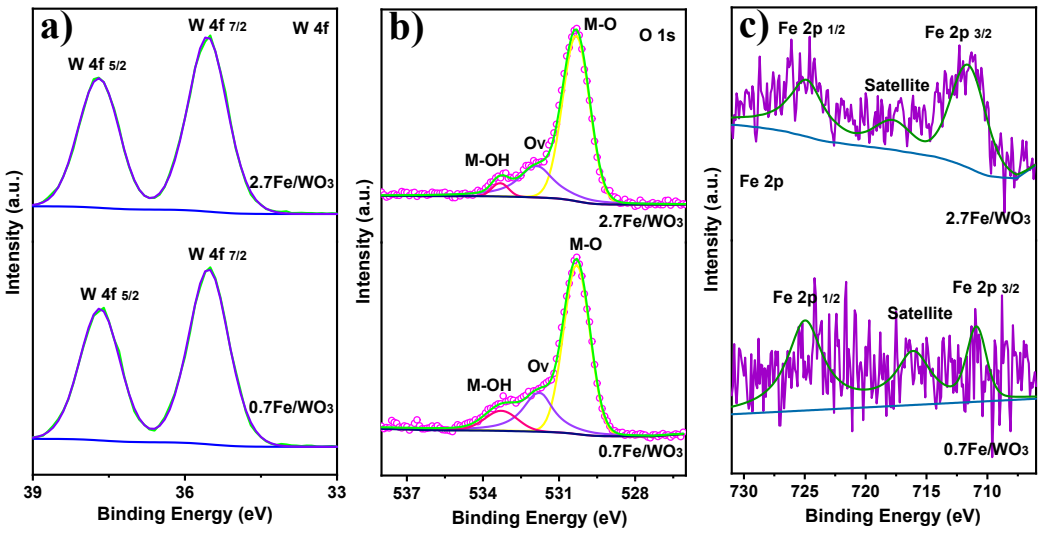

Fig. S4. XPS spectra of $0.7Fe/WO_3$ and $2.7Fe/WO_3$: a) W 4f, b) O 1s, and c) Fe 2p.

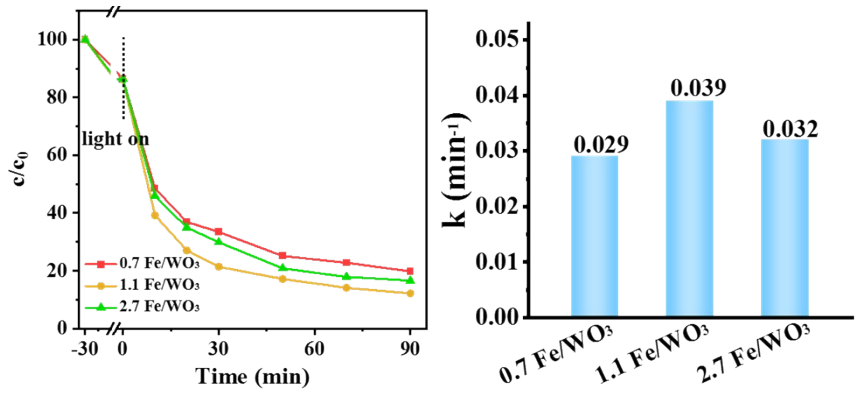

Fig. S5. Concentration vs time curves evaluated in the batch reactor system and corresponding k value of tetracycline (TC) degradation over Fe/WO_3 catalysts in the photo−Fenton system. Conditions are given in the Experimental part of the paper. k-values were determined from the initial rate data assuming a first-order reaction r = k c, where c is the TC concentration. Experimental condition: 10 mg of catalyst, 100 mL 20 mg_{TC} L^{-1}, 20 mmol of H_2O_2 (30 wt%) solution.

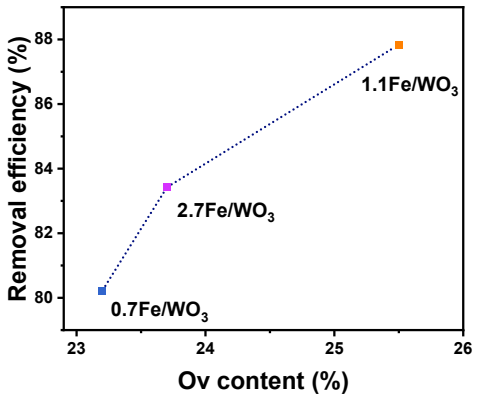

Fig. S6. Relationship between the removal efficiency of TC and the concentration of surface Ov of Fe/WO_3 catalysts with different Fe loading. Determined by XPS.

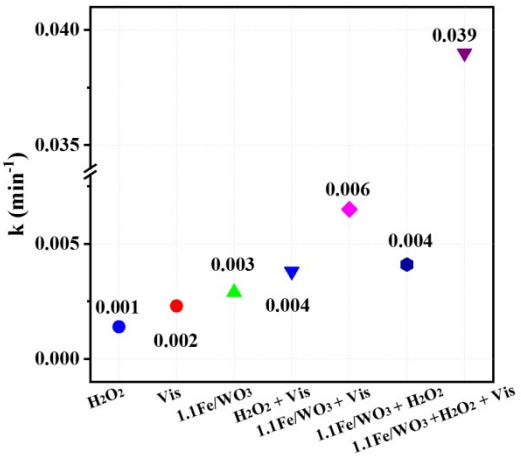

Fig. S7. Influence of different degradation conditions reflected by k-values of the photo-Fenton system. Experimental condition: 10 mg of catalyst, 100 mL of 20 mg_{TC} L^{-1}, 20 mmol of H_2O_2 (30 wt%) solution.

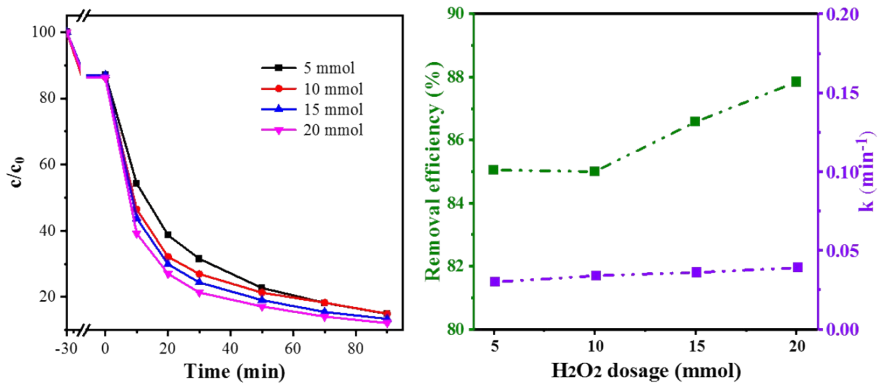

Fig. S8. TC removal curves over 1.1Fe/WO_3 in the photo−Fenton system using different H_2O_2 content. Experimental condition: 10 mg of catalyst, 100 mL of 20 mg_{TC} L^{-1}, 30 wt% H_2O_2 solution.

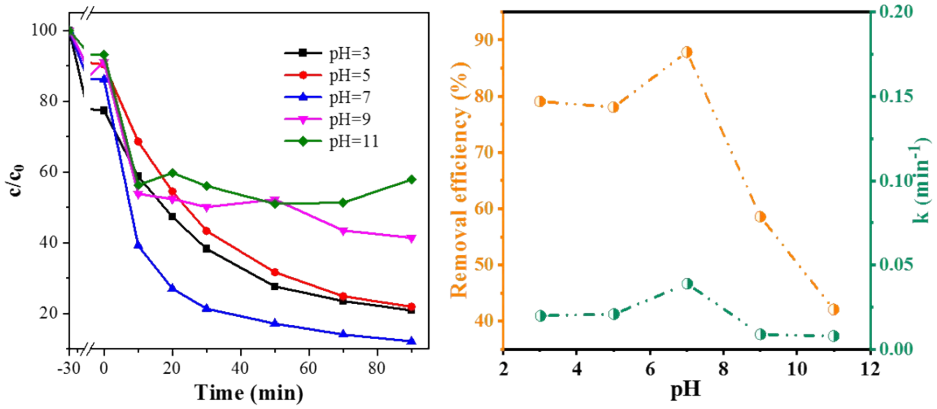

Fig. S9. TC removal curves over 1.1Fe/WO_3 under different pH in the photo−Fenton system. Experimental condition: 10 mg of catalyst, 100 mL 20 mg_{TC} L^{-1}, 20 mmol of H_2O_2 (30 wt%) solution. The solution pH was adjusted by 0.1 M HCl or 0.1 M NaOH solutions.

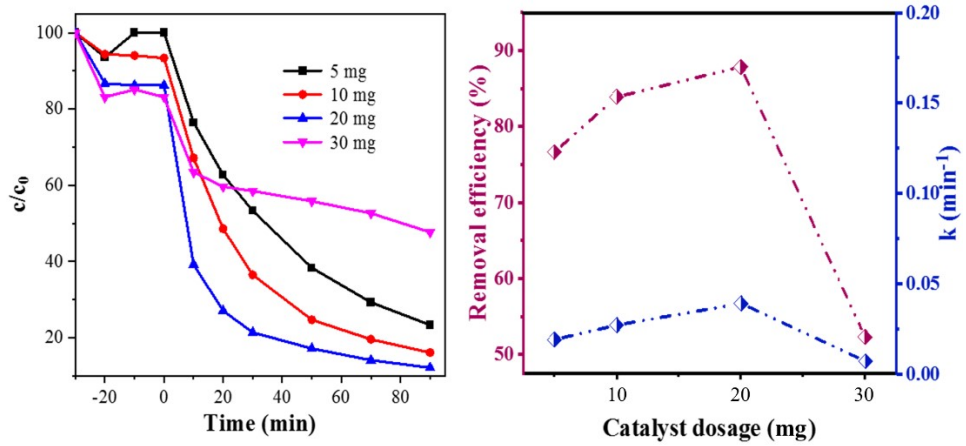

Fig. S10. TC removal curves of over 1.1Fe/WO_3 with different catalyst dosages in the photo−Fenton system. Experimental condition: 100 mL of 20 mg_{TC} L^{-1}, 20 mmol of H_2O_2 (30 wt%) solution.

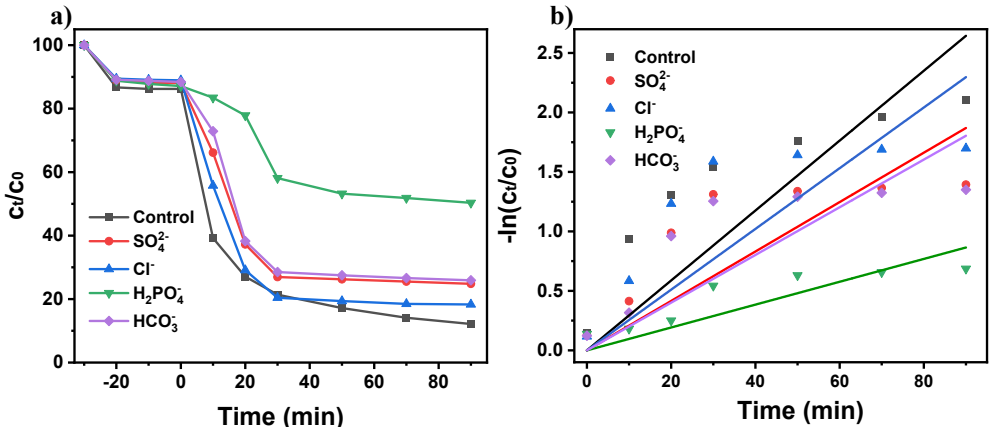

Fig. S11. TC removal curves of over 1.1Fe/WO_3 with different anions in the photo−Fenton system. Experimental condition: 100 mL of 20 mg_{TC} L^{-1}, 20 mmol of H_2O_2 (30 wt%) solution, 1mmol anions.

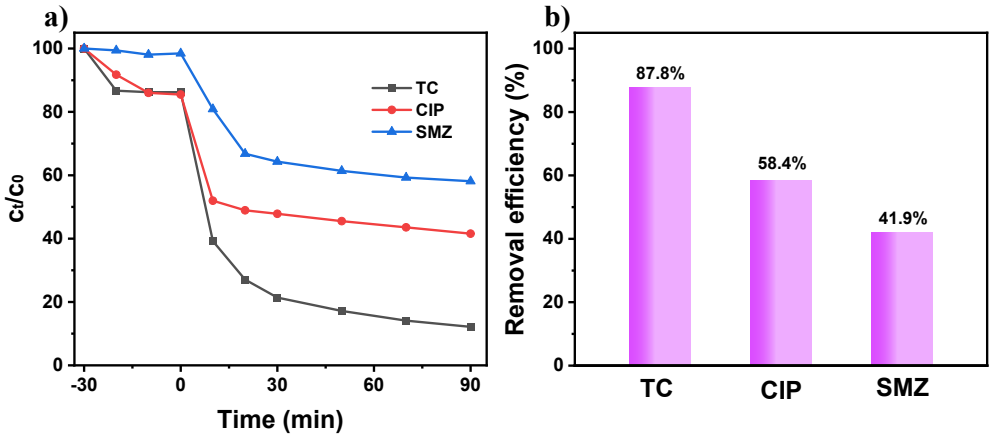

Fig. S12. Different antibiotic pollutants removal curves of over 1.1Fe/WO_3 in the photo−Fenton system. Experimental condition: 100 mL of 20 mg_{TC} L^{-1}, 100 mL of 5 mg_{CIP} L^{-1}, 100 mL of 20 mg_{SMZ} L^{-1}, 20 mmol of H_2O_2 (30 wt%) solution.

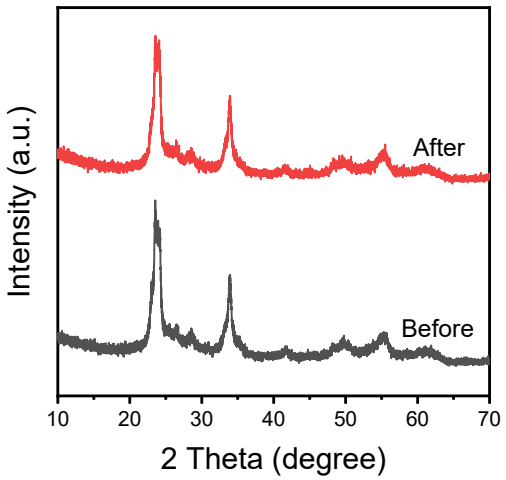

Fig. S13. XRD patterns of 1.1Fe/WO_3 before and after TC removal reaction in photo−Fenton system.

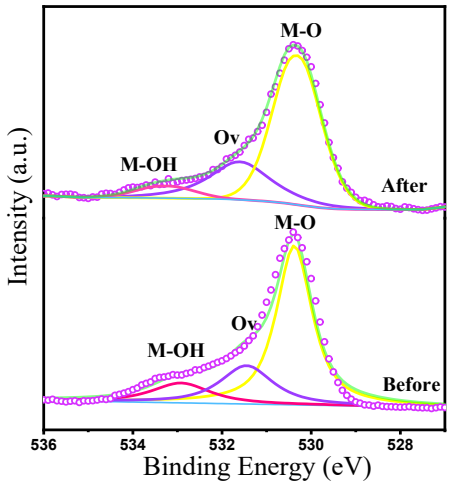

Fig. S14. XPS spectra of 1.1Fe/WO_3 before and after TC removal reaction in photo−Fenton system.

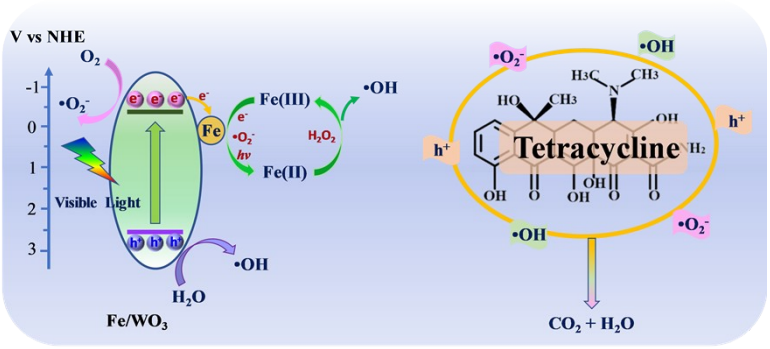

Fig. S15. Diagram illustrating the proposed photo-Fenton catalytic tetracycline degradation mechanism over Fe/WO_3.

Possible degradation pathways of TC and toxicity analysis

To further investigate the degradation pathways of tetracycline, HPLC-MS was used to identify intermediates. Three possible degradation pathways are proposed and shown in Fig. S10 (a). In pathway I, two hydroxyl groups are added to tetracycline in the first step to form P1 (*m/z* 476), which then produces P2 (*m/z* 354) via dehydration, oxidation, and N-methylation. P2 then forms P3 (*m/z* 288) through dehydration and ring opening. In pathway II, tetracycline is first decomposed to P4 (*m/z* 427) via dehydration, then further degraded to P5 (*m/z* 395) and P6 (*m/z* 297). In pathway III, P7 (*m/z* 417) is produced through demethylation oxidation. Subsequently, P8 (*m/z* 388) and P9 (*m/z* 319) are generated via dehydration, deamidation, and ring opening. These intermediates (P3, P6, and P9) gradually oxidize to smaller molecules by active species,

resulting in the formation of P10, P11, P12, and P13 with *m/z* values of 170, 194, 197, and 90, respectively. Ultimately, these small molecule intermediates are further decomposed and fully mineralized to CO_2 and H_2O.

Predicting these intermediates' toxicity and potential environmental hazards is crucial to assess the degradation system's effectiveness The toxicity of these intermediates is evaluated using the ECOSAR procedure in the EPI Suite software, along with developmental toxicity values for fish, Daphnia, and green algae As shown in Fig. S10 (b), the toxicity of the initial intermediates to the three reference organisms is higher than that of TC, which is then converted into environmentally benign substances after deep degradation in pathway I. The developmental toxicity values of the intermediates decrease, except for P4 and P9 in pathways II and III. However, it is worth noting that these elevated values occur in the early stages of degradation and are likely eliminated in subsequent reaction steps.

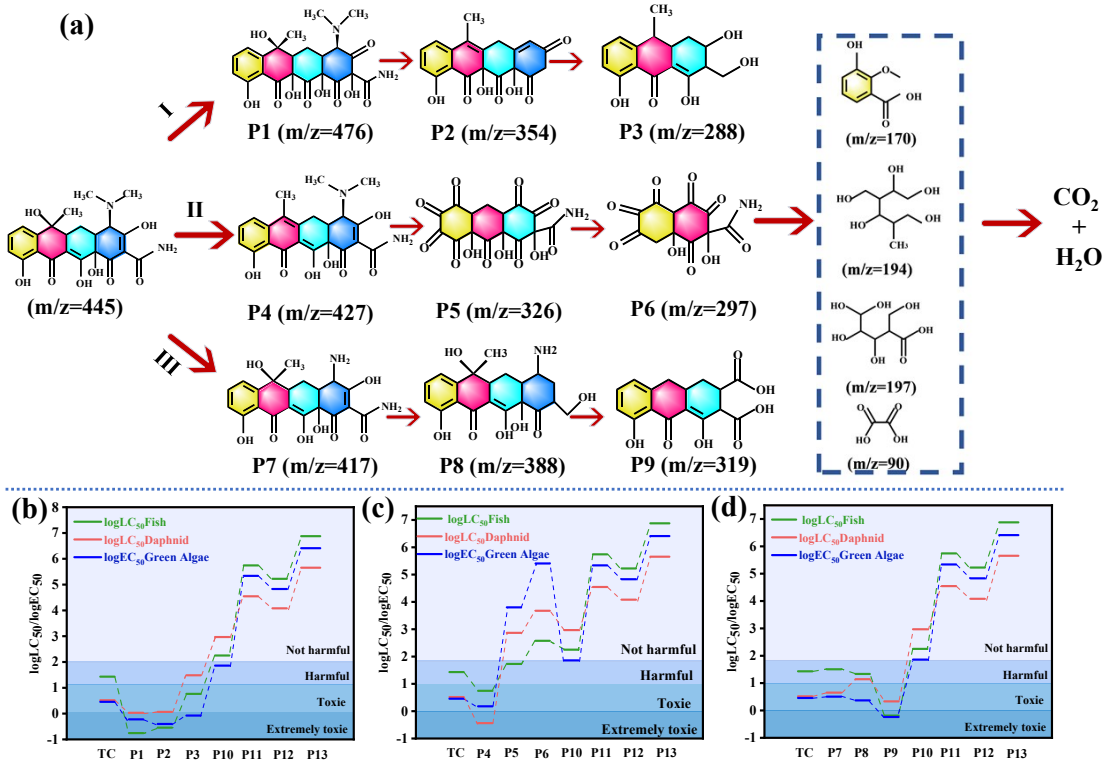

Fig. S16. (a) Plausible pathway for catalytic degradation of tetracycline over Fe/WO_3 in photo-Fenton system. (b-d) Acute toxicity analysis of tetracycline and the intermediates to three aquatic organisms.

Table S1. Properties of Fe/WO_3. The Fe content was estimated using the ICP-OES method.

Sample	S_{BET} (m^2/g)	Pore volume (cm^3/g)	Pore size (nm)	Fe content
WO_3	28.0	0.31	43.9	--
$0.7Fe/WO_3$	27.1	0.24	35.0	0.7%
$1.1Fe/WO_3$	32.0	0.26	37.1	1.1%
$2.7Fe/WO_3$	23.9	0.22	32.2	2.7%

Table S2. EXAFS parameters of the samples.

Sample	Shell	Bond length (Å)	Coordination Number (CN)	σ^2 ($Å^2$)	E_0 shift (eV)	R-factor
Fe foil	Fe-Fe	2.47±0.01	8*	0.007±0.001	5.4±2.0	0.016
	Fe-Fe	2.85±0.01	6*	0.007±0.002		
$1.1Fe/WO_3$	Fe-O	1.99±0.01	4.4±0.6	0.009±0.002	-2.9±1.7	0.017

The value of amplitude reduction factor (S_0^2) lines between 0.7 and 1. Bond length is the interatomic distance. σ^2 is Debye-Waller factor (a measure of thermal and static disorder in absorber scatter distance). E_0 shift is edge-energy shift (the difference between zero kinetic energy value of sample and that of the theoretical model). R factor is used to evaluate the goodness of fit.

Table S3. Chronic Toxicity of TC and its intermediates as assessed using the ECOSAR program.

Compound	Fish (LC_{50})	Daphnid (LC_{50})	Green Algae (EC_{50})
TC (*m/z*) = 445	27.08	2.87	3.30
P1 (*m/z*) = 476	0.18	0.60	1.08
P2 (*m/z*) = 354	0.29	0.40	1.17
P3 (*m/z*) = 288	5.80	0.84	30.63
P4 (*m/z*) = 427	5.57	1.51	0.37
P5 (*m/z*) = 395	53.64	6308.12	735.53
P6 (*m/z*) = 297	377.75	255976.4	4727.157
P7 (*m/z*) = 417	32.04	3.21	4.48
P8 (*m/z*) = 387	21.63	2.34	13.93
P9 (*m/z*) = 319	0.65	0.58	2.15
P10 (*m/z*) = 170	178.67	72.60	931.13
P11 (*m/z*) = 194	552968	217971.6	35180.3
P12 (*m/z*) = 197	167957.7	67473.0	12070.4
P13 (*m/z*) = 90	7539976.6	2578042.1	450993.2